

AN APPRAISAL OF THE MASS TRANSFER EFFICIENCY OF DISTRIBUTED BUBBLE SIZES IN A STIRRED FERMENTER

D.S Vlaev^a, S.D.Vlaev^b and R Mann^a

*a School of Chemical Engineering and Analytical Science
The University of Manchester, Manchester, M60 1QD, UK; r.mann@manchester.ac.uk*
*b Institute of Chemical Engineering,
Bulgarian Academy of Sciences, Sofia, Bulgaria*

Abstract A simplified CFD based on networks of zones has been applied to an industrial stirred bio-reactor. Feed gas is dispersed axi-symmetrically around the lowest impeller into 10 sizes from 0.1 to 100mm. The bubbles are treated as non-coalescing in the high ionic strength high viscosity fermentation liquor. Detailed results of the spatial variation of gas hold-up, bubble oxygen compositions and dissolved oxygen saturation are presented for the 96th hour in a seven-day batch. The model predictions match the key overall operational values of 17% gas hold-up, 17.3% O₂ in the exit gas (air being fed at 21%) and 36% O₂ saturation close to the lowest impeller. There are significant spatial non-uniformities. Bubbles outside the range of 1-10 mm are shown to be inefficient for mass transfer. Dissolved oxygen saturation varies from a maximum of 44% to just 4%, which may be detrimental for the vitality of the microbes.

Key words: Fluid mixing, stirred vessel, mass transfer, bio-reaction, bubble size distribution

1 INTRODUCTION

The bio-processing sector of chemicals manufacture has come under pressure from the Food and Drugs Administration (FDA) to improve its technology. Manufacturing units like the conventional “stirred bioreactor” are perceived as being unchanged for decades. The FDA is promulgating adoption of “Process Analytical Technology (PAT)” for innovation from “*better understanding of process fundamentals*”. Some classic texts wrongly oversimplify the stirred bioreactor and assume a spatially uniform environment. More recently, it has been recognised that spatial gradients may exist simultaneously in multiple culture parameters [1]. Spatial non-uniformities present challenges for computational fluid dynamics (CFD). Early work established a hierarchy of Eulerian-Lagrangian combinations[2]. More recent studies have been restricted to the physical aspects of gas-liquid bubbly flow, often with simplifications. Extension to include large eddy effects further stretches computing power. The adding in of mass transfer with bio-reaction is still demanding for CFD [3]. One alternative to avoiding computer intensive rigorous solutions to the (multi-phase multi-component) Navier-Stokes equations is to use (relatively) large sets of backmixed zones/cells. These are configured to accommodate close approximations to liquid circulatory flow and associated turbulence. Initially developed and applied to bioreactors with axi-symmetry (2-D) [4,5], the approach was extended to 3-D, thus allowing for point-wise nutrient addition or (faulty) asymmetric gas injection [6]. Computation of bioreactors to include the effects of distributed bubble sizes remains challenging. The importance of this factor can be judged from an early observation [7] that in bubble columns with viscous fluids, very small bubbles disengaged only slowly and became depleted of oxygen, thus not contributing to mass

transfer. The same can happen in stirred vessels where higher shear rates exist [8]. Most recent CFD applications apply some sort of simplification to ameliorate computational demand, including the method of moments, leaving out the bio-reaction and compartmentalisation [9, 10, 11]. It is the purpose of this paper to examine distributed bubble size effects, using a simplified computationally tractable CFD based on networks-of zones (NoZ).

2 DETAILS OF THE TRIPLE_IMPELLER FERMENTER

Details of the fermentation process and the associated input operational parameters have been fully reported in our earlier paper for the same fermentation but with a single bubble size [4]. The 3m³ triple impeller fermenter, with dimensions shown in Fig.1, has 3 eight-bladed Rushton turbines with D=0.52m rotating at 3rps. Three key parameters are the overall gas hold-up (voidage), the off-gas oxygen composition and the dissolved oxygen adjacent to the lowest impeller. These three key parameters were monitored throughout a 7-day batch (Fig. 2.). The NoZ analysis will predict the details of the spatial pattern of behaviour at the 96th hour of operation.

3 THE NETWORKS-OF-ZONES (NoZ) THEORY

The networks-of-zones theory has been explained previously in detail (4, 5, 6) and only an update is presented here. Briefly, the theory sets up an overall convective liquid flow driven by each impeller in accordance with established flow numbers using: $Q_L = KND^3$. This convective liquid flow is conserved axi-symmetrically in 2-D and set in concentric toroidal nested flow loops with each loop liquid flow given by: $q_L = Q_L / 2n$, each overall impeller flow is contained within $2 \times (n \times n)$ networks, one $(n \times n)$ above and below each impeller. Turbulent exchange is represented by an equal and opposite lateral exchange flow between adjacent zones related to the local loop flow and given by (+ and -) βq_L . Gas bubbles of specified size are ejected from the impeller periphery with a given injection rate by number matching the gas feed rate. The injected bubbles respond to the liquid flow pattern by a resultant combination of rise by buoyancy and vertical/horizontal convection governed by the axial/radial liquid flow pattern. Behaviour as a fermenter then requires the combination of mass transfer and bio-reaction. This networks-of-zones theory has already been applied for a single bubble size of 5mm and is now extended for a distribution of bubble sizes for a “3 x [2 x (10 x 10)]” axi-symmetric 2-D assembly of 600 zones.

4 ANALYSIS OF DISTRIBUTED BUBBLE SIZE

4.1 Underlying principles

Three parameters are needed to exactly match the predictions to the pilot plant measurements, namely: bubble rise velocity u_b , mass transfer coefficient k_L and reaction speed via a (pseudo) first order rate constant k_1 . This analysis is readily extended to distributed bubble sizes if for each bubble size the associated input gas flow rate allocated to that size is specified. The model thus envisages that streams of bubbles are created and ejected from the sparger/impeller region at a number frequency corresponding to each size, so that each size stream carries a given proportion of the overall feed rate of gas. Bubbles of each size will be entrained in and respond to the convective circulation flow and turbulence by rising buoyantly and circulating, eventually disengaging.

4.2 Bubble size distribution

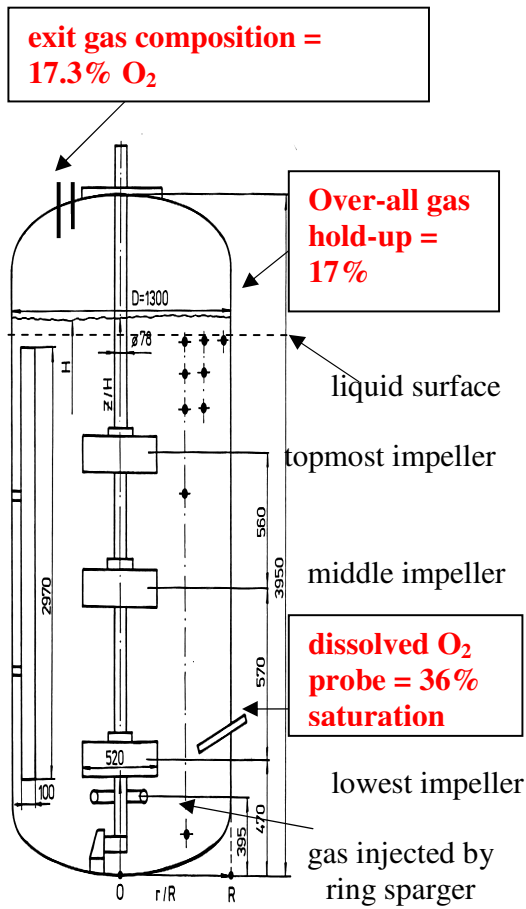


Fig. 1 Stirred fermenter details

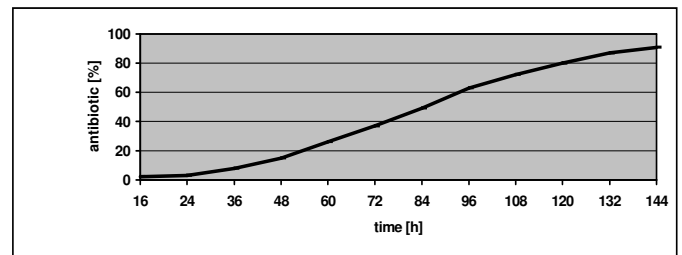
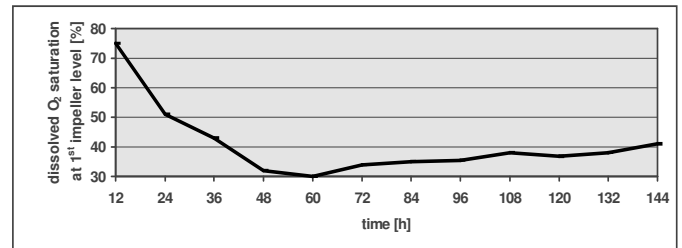
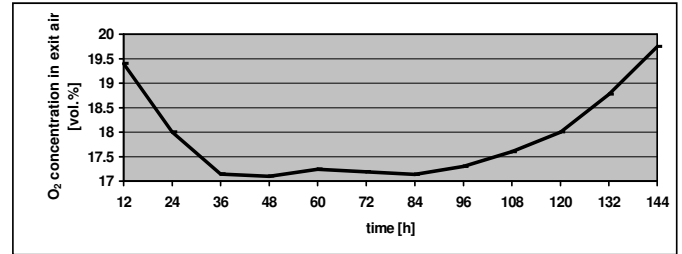


Fig.2 Monitoring through a 7-day batch

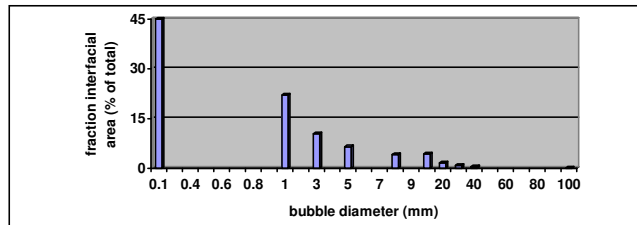
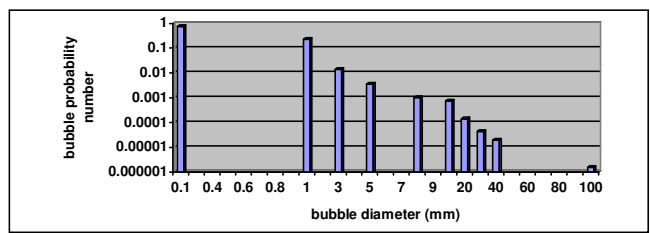
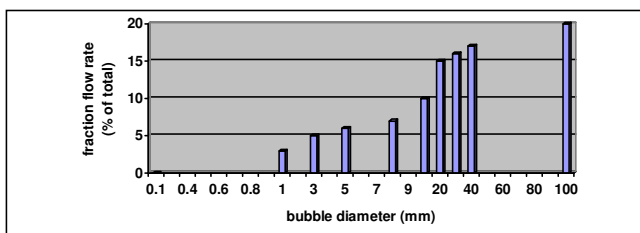


Fig.3 Bubble size distribution properties

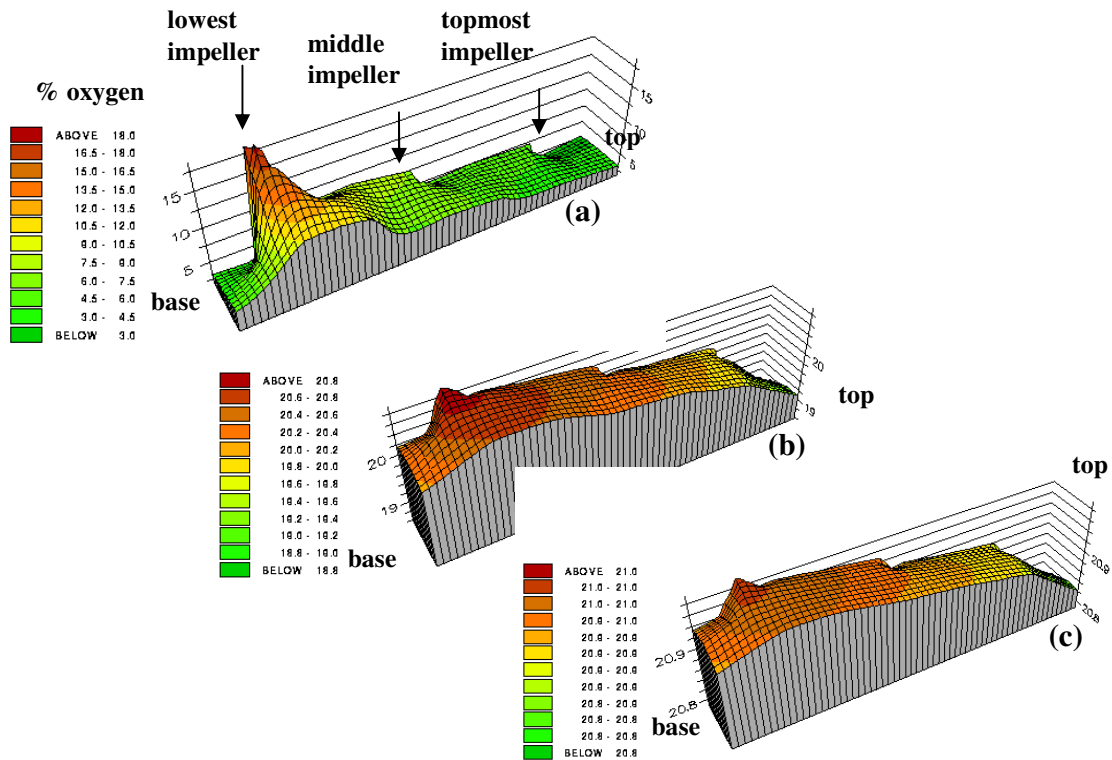
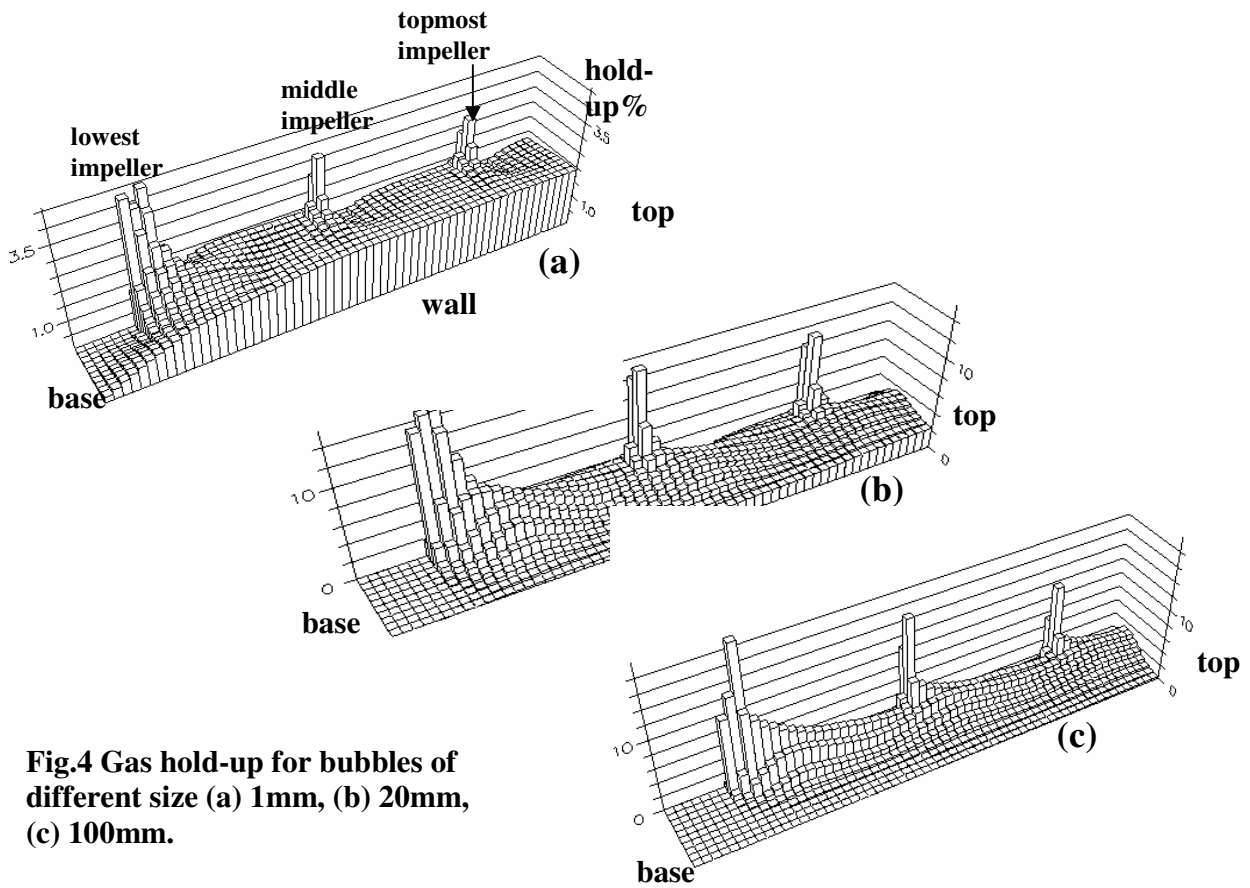
In order to model the industrial fermenter, a set of ten bubble sizes was chosen from 0.1 mm to 100 mm (with representative sizes of 0.1, 1, 3, 5, 8, 10, 20, 30, 40 and 100 mm as in Fig. 3) to encompass the expected range. Each size was allotted a flow proportion (Table.1) with the NoZ analysis giving an exact match to the overall 17% gas hold-up. These bubble flow allocations were estimated to be applicable at 96 hours elapsed time and were in line with measurements on a simulated fluid studied on the UMIST pilot plant. It is assumed that each cohort of bubbles of a given size are dispersed from the outer (toroidal) boundary of the impeller and that the system is non-coalescing so that all the bubbles remain intact once generated. This represents the extreme of complete segregation of bubbles of different size. Evidence for the basic correctness of this low coalescence scenario comes from the generation and extreme persistence of the tiny bubbles seen in fermenters, suggesting negligible rates of coalescence. Further properties of the bubbles are shown in Fig. 3. The number distribution shows a complete inversion of the flow, with a massive proportion of 0.1 mm bubbles. The frequency of appearance of the largest 100 mm bubbles is seven orders of magnitude smaller. There is a less pronounced effect for surface with the very tiny bubbles representing some 45% of the area. The 5 mm bubbles portion carries 7.5% of the overall area, whilst the 100 mm bubbles comprise only 0.1% of surface.

4.3 Gas hold-up predictions

The injected bubbles can now be tracked according to how they respond to the pattern of convective re-circulation and associated turbulent exchange. The results for gas hold-up in each zone for a 3x (2x(10x10)) network are shown for three bubble sizes in Fig. 4. The pattern of the contribution to gas-hold up for each bubble size is the result of interactions of rise velocity with the axial up- and down-flows and the radial in- and out-ward flows.. In Fig. 4(a), due to the very low rise velocity, above the lowest impeller the hold-up is more uniform and close to 2% although with noticeable local peak values where uprising bubbles converge with the out-ward impeller flow just below each impeller, though this effect diminishes for the higher impellers. The other noticeable effect is below the bottom impeller where small bubbles are being convected downwards. In Fig. 4(b), the faster rising 20 mm bubbles contribute more to the overall hold up but with a larger spatial variation in distributed local hold-up values. These larger bubbles rise too rapidly for any hold-up to be generated underneath the bottom impeller. The peak values at each impeller diminish progressively for the middle and topmost impellers and the lowest values appear at the vessel walls. The pattern is similar for the very largest fastest rising 100 mm bubbles. Although the peak local value is higher at some 17% in this case, there are again no bubbles of this size below the bottom impeller and the hold-up due to this size is virtually zero at the outer wall. In other words, a visual inspection at the walls (say through a porthole/window) would show only smaller bubbles. Finally, it should be noted that the response of different bubble sizes to the impeller flows means that the locally observed bubble size distribution will vary with spatial position. The total gas hold-up in each zone is the addition of the contribution from each of the nine bubble fractions. The overall hold-up for the fermenter is the sum of the 600 zones which exactly matches the overall experimental value of 17%.

4.4 Mass transfer behaviour

The predicted mass transfer behaviour is shown in Fig. 5. The composition of the bubbles leaving from the surface set of zones determines the exit gas composition. A value of $k_L = 0.049 \text{ cm s}^{-1}$ predicts and matches the experimental 17.3% O₂ by volume. The smaller 1 mm bubbles exhibit a



gradual depletion of oxygen towards the surface as the microbes inspire oxygen. The exit composition for this size is 2.5%, showing a 90% O₂ depletion. The larger 20mm bubbles exit at close to 19% oxygen, with only 10% removal of oxygen. The 100mm bubble show a merely 1% depletion as they exit at 20.8% as a result of their faster rising velocity. Fig.6 shows in summary the overall behaviour for each bubble size set. From Fig. 6(a) the almost 90% abstraction of oxygen for the smallest 0.1 and 1mm bubbles declines with size. Combining the variation in flow rate with the depletion shows the bubbles in the mid-size perform optimally (Fig. 6(b)). Fig. 6 shows benefits from controlling bubble size.

The resulting liquid dissolved oxygen saturation is governed by the bio-reaction kinetics. A (pseudo)-1st-order constant of 0.28 s⁻¹ matches the experimental value to give the spatial field in Fig. 7(a). The fluid is relatively unsaturated with a highest value of 44% around the injection zone. Combination of bubble oxygen content and dissolved oxygen gives the field of absorption fluxes in Fig. 7(b). The injection region shows a “flame” of high values, although most zones show low fluxes around one-tenth of the peak value.

4.5 Behaviour of k_L during the batch

Although these results discussed in detail refer to a single instant during the batch (96 hrs), the basic parameters vary through the batch. Matching with fermenter monitoring is shown in Fig 8 for both single and distributed bubble size cases. The k_L values decline with time, reflecting the increase in viscosity. For distributed bubble size, a higher value of k_L has to be applied to compensate for the reduced absorption efficiency of the very smallest and largest bubbles.

5 CONCLUSIONS

An earlier analysis of an industrial bio-reactor modelled by networks-of-zones[4] has been extended to distributed bubble sizes. The spatial gas hold-up due to each bubble size shows a different pattern. Only very small bubbles disperse below the lowest impeller. In contrast, the larger faster rising bubbles re-circulate less and rise predominantly mid-way between the wall and impeller shaft. The individual zone bubble size distribution will thus vary with zonal position. The smaller bubbles (<1) mm are heavily depleted of oxygen and occupy hold-up without contributing to mass transfer, whereas the large bubbles (> 10mm) have very low depletion. Bubbles in the 1-10mm range are most efficient. Dissolved oxygen is assessed at a maximum of 44% of saturation at the lowest impeller and falls as low as 4% beneath it. Most of the fermenter has less than 20% O₂ saturation, which may not be ideal for aerobic metabolism.

6 NOMENCLATURE

D	impeller diameter	N	impeller rotation speed
K	impeller flow constant	T	vessel diameter
d_b	bubble size	Q_L	overall impeller flow rate
i	axial zone position	q_L	(nested) loop flow
j	radial zone position	u_b	bubble rise velocity
k_L	mass transfer coefficient	β	turbulent exchange parameter
k_1	(pseudo) 1 st order bioreaction rate constant	ϵ_G	gas hold-up

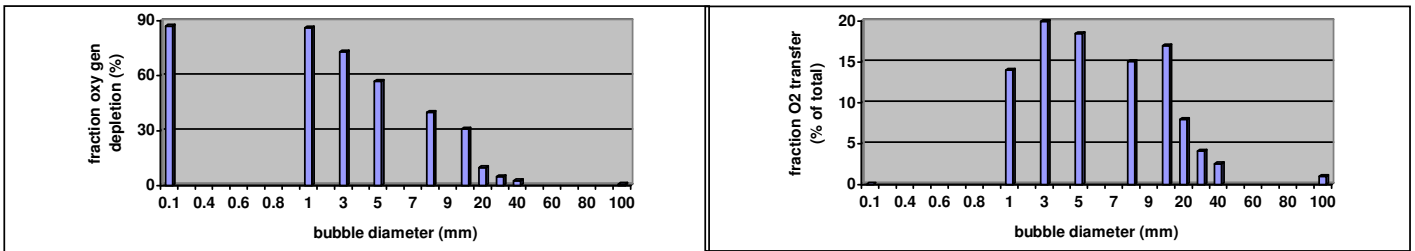


Fig.6 Bubble oxygen depletion and overall contribution to absorption of oxygen

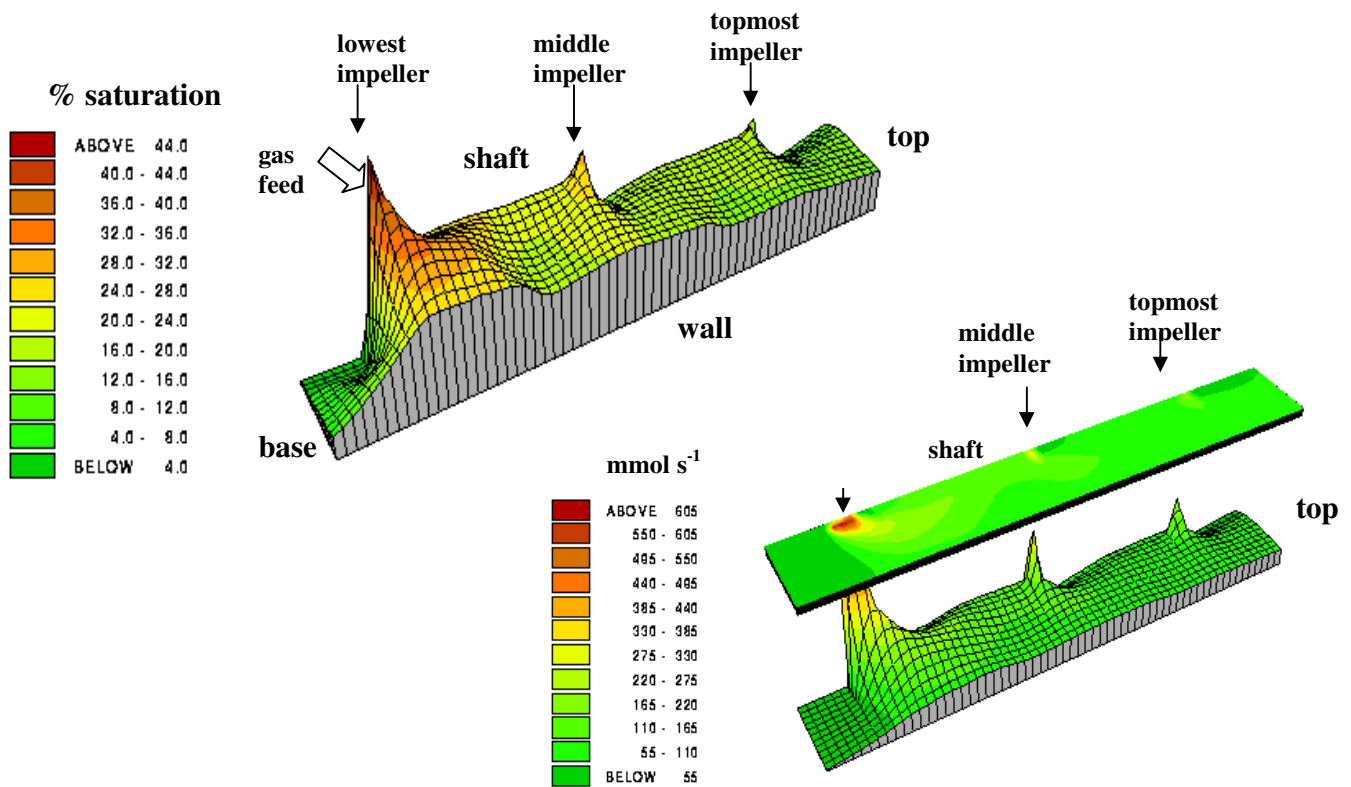


Fig.7 Spatial fields of dissolved O₂ saturation and local O₂ fluxes

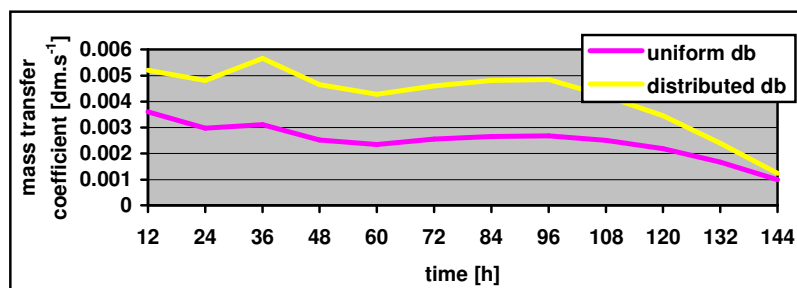


Fig.8 Variation of mass transfer coefficient through the batch

REFERENCES

- [1] Lara, A.R., Galindo, E., Ramirez, O.T. and Palomares, L.A., 2006, "Living with heterogeneities in bioreactors: Understanding the effects of environmental gradients on cells", *Molecular Biology*, 34(3), 1073-1085.
- [2] Delnoij, E., Kuipers, J. A. M. and van Swaaij, W. P. M., 1997, "Computational fluid dynamics applied to gas liquid contactors", *Chem. Eng. Sci.*, 52, 3623-3638.
- [3] Elqotbi, M., Montastruc, L., Vlaev, S.D and Nikov, I., 2006, "CFD simulation of gluconic acid production in a stirred gas-liquid fermenter", *Proc. 12th Europ. Conf. on Mixing*.
- [4] Vlaev, V., Mann, R., Lossev, V., Vlaev, S.D., Zahradnik, J. and Seichter, P., 2000, "Macro-mixing and streptomyces fradiae: Modelling oxygen and nutrient segregation in an industrial bioreactor", *Trans. I. Chem. E.*, 78(A), 354-362.
- [5] Hristov, H.V., Mann, R., Lossev, V. and Vlaev, S.D. and Seichter, P., 2001, "A 3-D analysis of gas-liquid mixing, mass transfer and bioreaction in a stirred bioreactor", *Trans. I. Chem. E.*, 79(C), 232-241.
- [6] Hristov, H.V., Mann, R., Lossev, V. and Vlaev, S.D.,2004,"A simplified CFD for 3-D analysis of fluid mixing, mass transfer and bioreaction in a fermenter equipped with triple novel geometry impellers", *Trans. I. Chem. E.*, Part(C), 82(C1),21-34.
- [7] Muller F. L. and Davidson, J. F., 1992, "On the contribution of small bubbles to mass transfer in bubble columns containing high viscosity liquids", *Chem. Eng. Sci.*, 47, 3525-3532.
- [8] Khare, A.S. and Niranjana, K., 1995, "Impeller-agitated aerobic reactor: The influence of tiny bubbles on mass transfer", *Chem. Eng. Sci.*, 50, 1091-1105.
- [9] Schutze, J. and Hengstler, J., 2006, "Assessing aerated bioreactor performance using CFD", *12th Europ. Conf. on Mixing*.
- [10] Dhanasekharan, K. M., Sanyal, J., Jain, A. and Hadari, A., 2005, "A generalised approach to model oxygen transfer in bioreactors using population balances and computational fluid dynamics", *Chem. Eng. Sci.*, 60, 213-218.
- [11] Laakkonen, M., Moilanen, P., Alopaeus, V. and Aittamaa, J, 2007, "Modelling local gas-liquid mass transfer in agitated vessels", *Trans. I. Chem. E.*, 85(A5), 665-675.

Table 1: Bubble size properties and flow statistics

Bubble rise velocities and flow allocations										
$d_b(\text{mm})$	0.1	1	3	5	9	10	20	30	40	100
$u_b(d_b)(\text{cm s}^{-1})$	0.1	6	7	8	9	10	20	30	40	50
% of flow	~0	3	5	6	7	10	15	16	17	21
		8		23			69			
Khare and Niranjana [8] - small stirred tank T=0.3 m										
$d_b(\text{mm})$	<3			3 –100						
% of flow	1-29			61-99						
% of hold-up	up to 70			more than 30						